Splitting of Ni 3*d* states at the surface of NiO nanostructures

L. Soriano, A. Gutiérrez, I. Preda, S. Palacín, and J. M. Sanz
Departamento de Física Aplicada C-XII, Instituto de Ciencia de Materiales Nicolás Cabrera, Universidad Autónoma de Madrid, Cantoblanco E-28049 Madrid, Spain

M. Abbate
Departamento de Física, Universidade Federal do Paraná, Caixa Postal 19091, 81531-990 Curitiba PR, Brazil

J. F. Trigo
Departamento de Energía, CIEMAT, Avda. Complutense 22, E-28040 Madrid, Spain

A. Vollmer and P. R. Bressler
BESSY, Albert Einstein Strasse 15, D-12489 Berlin, Germany
(Received 17 April 2006; revised manuscript received 30 May 2006; published 2 November 2006)

The electronic structure of NiO nanometric planar islands on highly oriented pyrolitic graphite has been studied by means of the Ni 2*p* and O 1*s* x-ray absorption spectra. The O 1*s* spectrum of the early stages of growth shows a double peak at threshold which is attributed to a splitting of the unoccupied Ni e_g states. This spectrum is compared to previous results for 3 nm NiO nanoparticles which also show a rather similar splitting of the Ni e_g states. This splitting observed in the O 1*s* spectra of the NiO nanostructures is caused by the reduced symmetry of the Ni ions at the surface. Cluster model calculations for a high-spin Ni^{2+} ion performed in both octahedral (bulk) and pyramidal (surface) symmetries confirm this interpretation. This new interpretation of the surface electronic structure of NiO suggests a revision of the accepted concepts concerning this system.

DOI: 10.1103/PhysRevB.74.193402 PACS number(s): 78.70.Dm, 73.20.At, 79.60.Jv

This work deals with the study of the electronic structure of the NiO nanostructures formed at the early stages of growth of NiO on highly oriented pyrolytic graphite (HOPG). Our main aim is the study of nanostructured NiO systems where possible surface effects are enhanced by the relatively large surface-to-volume ratio of the nanostructures. In fact, previous studies[1] of 3 nm NiO nanoparticles, with unique catalytic properties, revealed a splitting of the unoccupied Ni e_g states, as shown by the O 1*s* XAS spectra. This splitting was interpreted as the result of the lack of the apical oxygen at the NiO surface and the large surface-to-volume ratio of the nanoparticles.[1] The early stages of growth of NiO on HOPG are known to produce planar NiO islands along the graphite steps as shown by atomic force microscopy (AFM) images.[2] Such a particular arrangement of NiO nanostructures possesses a relatively large surface-to-volume ratio and is expected to exhibit similar surface effects as in the NiO nanoparticles. In this work, we present new data and calculations confirming this picture. We show below that the Ni atoms located at the surface of the planar islands formed at the early stages of growth of NiO/HOPG present the same splitting of the e_g states as the nanoparticles. Furthermore, the splitting in the O 1*s* XAS edge can be reproduced by means of cluster model calculations in both octahedral (bulk) and pyramidal (surface) symmetries. These calculations show that, for pyramidal symmetry, the e_g band splits into the z^2 and x^2-y^2 states. The calculated energy splitting and intensity ratio of the subbands can successfully reproduce the experimental data of the NiO nanostructures. These new results might help to explain the unique catalytic properties of the NiO nanoparticles[3] as, according to these results, a z^2 dangling bond is produced at the surface of the NiO nanostructures.

The electronic structure and the nature of the band gap of NiO has been a matter of controversy for years.[4–8] It has been studied not only as bulk material but also as highly dispersed nanostructures, due to its catalytic properties. For instance, 3 nm NiO nanoparticles showed unique catalytic properties in the oxidation of carbon monoxide and other species.[3] In these systems, the nature and properties of the defects and their influence on the electronic structure are still open questions. These enhanced catalytic properties of the NiO nanoparticles were attributed to the presence of highly oxidized Ni^{3+} species.[9] A posterior study of these nanoparticles using Ni 2*p* XAS showed unambiguously high-spin Ni^{2+} species.[1] This conclusion on the oxidation state of the Ni ions was also in agreement with previous studies of hole-doped $Li_xNi_{1-x}O$.[10,11] Furthermore, as mentioned above, the O 1*s* XAS spectra of the NiO nanoparticles showed a distinct splitting of the Ni e_g states. Other experimental and theoretical works on NiO (100) surfaces also predict surface states to be different from bulk states.[12–15] Other works concerning the influence of defects on the electronic structure of NiO and NiO surfaces can be found elsewhere.[16–19]

We have previously studied the early stages of growth of NiO/HOPG by Atomic Force Microscopy (AFM).[2] The AFM images revealed that NiO nucleates by forming a chain of planar islands along the HOPG steps. The planar islands are pollycrystalline and approximately circular, with a diameter of about 100 nm and a thickness of 3–10 nm. The previous AFM results show that the size distribution is relatively small. Such a quasi-bidimensional system exhibits a large surface-to-volume ratio in which possible surface effects are expected to be observed. Other related works on the growth of NiO on different substrates include NiO/MgO,[20,21] NiO/Cu,[22] and NiO/Pd.[23]

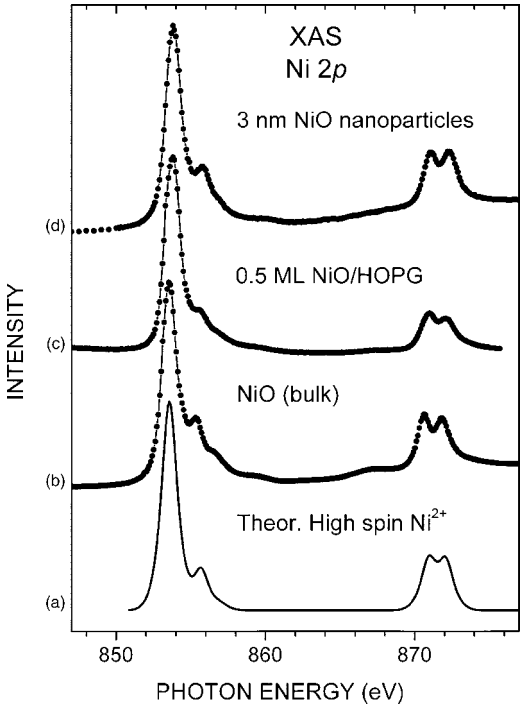

FIG. 1. (a) Atomic multiplet calculations for a high-spin Ni^{2+} ion with $10Dq=1.8$ eV; Experimental Ni $2p$ XAS spectra for (b) large NiO coverage (bulk); (c) 0.5 ML NiO/HOPG; and (d) 3 nm NiO nanoparticles.

NiO was deposited on HOPG by reactive evaporation from a pure Ni filament in the preparation chamber. The HOPG substrate was cleaved in air just before being introduced in the preparation chamber with a base pressure of $\sim 10^{-9}$ Torr. Then, it was thermally annealed in UHV at 300 °C to remove any possible surface contamination. The evaporation was performed in an oxygen atmosphere (5×10^{-5} Torr), with the substrate kept at room temperature. The oxygen gas was aimed directly to the sample using a narrow pipe to enhance the oxidation efficiency. The evaporation rate was maintained low enough to study the early stages of NiO growth in more detail.

XAS measurements were performed using the PM4 plane grating monochromator at the BESSY II storage ring (Berlin). The optical arrangement of this monochromator was set to optimize both the photon flux and the energy resolution, in order to obtain an acceptable signal from a very small amount of NiO. The estimated overall resolution was better than 100 meV at 530 eV. The spectra were collected in the total electron yield detection mode. In order to observe possible dichroism effects, the spectra were measured at normal and grazing angles. The spectra were normalized to the I_0 current, measured from a clean gold sample, to correct for the beam current. The NiO coverage was calculated from the O $1s$ XAS intensities following conventional methods described elsewhere.[24] Since the growth of NiO on HOPG is not in a layer-by-layer mode, the estimated coverages should be understood as the equivalent material to form a monolayer.

Figure 1 shows the Ni $2p$ XAS spectra of (b) large NiO coverages (bulk), (c) low NiO coverages (0.5 ML), and (d) 3 nm NiO nanoparticles, taken from Ref. 1. The spectrum for large NiO coverages (bulk) is in very good agreement with previous spectra for bulk NiO.[1] The $L_{2,3}$ absorption edge of the $3d$ transition metals is a powerful tool in the determination of the metal chemical state.[25] The Ni $2p$ XAS spectrum of NiO corresponds to $2p^6 3d^8 \rightarrow 2p^5 3d^9$ transitions which are dominated by multiplet effects. The multiplets are very sensitive to the ground-state symmetry and the crystal field.[25] The spectra are split by spin-orbit effects into the Ni $2p_{3/2}$(about 854 eV) and the Ni $2p_{1/2}$ (around 872 eV) regions. The corresponding atomic-multiplet calculations for high-spin Ni^{2+} ion is shown in Fig. 1(a). The crystal field parameter was set to $10Dq=1.8$ eV and the interactions were scaled down 80%. The comparison shows clearly that all the spectra correspond to high-spin Ni^{2+} species. The spectra of the 0.5 ML NiO/HOPG and the 3 nm NiO nanoparticles show a few minor changes. These changes can be explained in terms of a decrease of the crystal field at the surface.[26] Thus we conclude that the Ni cations of the NiO nanostructures are present in the high-spin Ni^{2+} form.

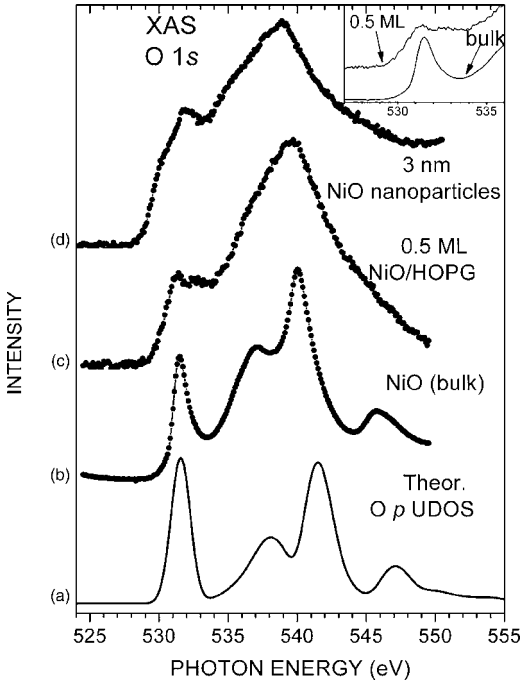

FIG. 2. (a) O $2p$ unoccupied density of states for antiferromagnetic NiO. Experimental O $1s$ XAS spectra for (b) large NiO coverage (bulk); (c) 0.5 ML NiO/HOPG; and (d) 3 nm NiO nanoparticles. The inset shows the near edge region of (b) and (c).

Figure 2 shows the O $1s$ XAS spectra of (b) large NiO coverages (bulk), (c) low NiO coverages (0.5 ML), and (d) 3 nm NiO nanoparticles, taken from Ref. 1. The spectrum for large NiO coverages (bulk) is in very good agreement with previous spectra for bulk NiO.[10,27,28] This shows that stoichiometric NiO can be grown on HOPG at room temperature using this method. The O $1s$ XAS spectra correspond to transitions to unoccupied O p states in the conduction band. The spectra reflect, through the corresponding Ni-O hybridization, the unoccupied Ni bands. The O $2p$ unoccupied density of states (UDOS) for antiferromagnetic NiO, calculated with the LMTO method,[29] is shown in Fig. 2(a). The spec-

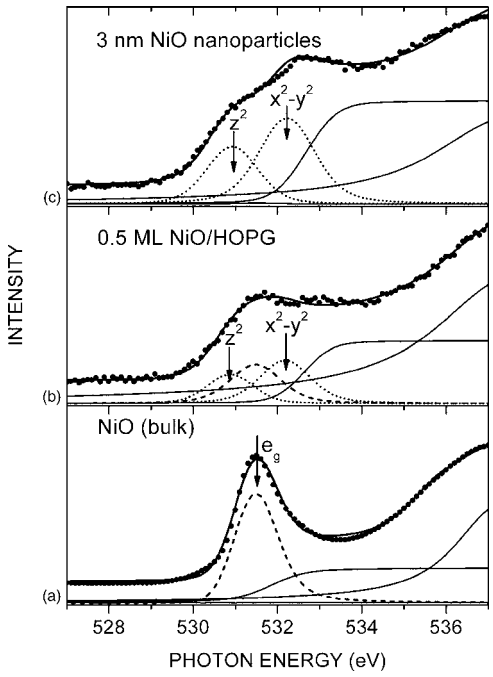

FIG. 3. Cluster model calculations of the near edge region of the O 1*s* XAS spectra and experimental O 1*s* XAS spectra (dots) for (a) large NiO coverage (bulk); (b) 0.5 ML NiO/HOPG; and (c) 3 nm NiO nanoparticles. Cluster model calculations in octahedral (short dash lines) and pyramidal symmetry (short dot lines). The solid lines represent typical curves used to fit the background.

trum of bulk NiO is in reasonably good agreement with the band structure calculation. The discrepancy in the energy position of the bands is attributed to self-energy effects beyond the usual LDA. The first peak in the O 1*s* XAS spectrum of bulk NiO, about 531.4 eV, is assigned to the unoccupied Ni e_g states. The peaks around 536.7 eV and about 540.5 eV correspond to O 2*p* character mixed with Ni 4*sp* states.

The spectrum for low NiO coverages (0.5 ML) presents significant differences with respect to that of bulk NiO. The mean probing depth of XAS at the O 1*s* edge is about 3 nm.[30] This value is smaller than the mean thickness of the NiO islands. Thus the O 1*s* XAS spectra taken at grazing incidence probe mostly the near surface region. The most relevant change in the spectra concerns the e_g region, which is shown in more detail in the inset of Fig. 2. The well defined e_g peak in bulk NiO is split in two broad and unresolved peaks for 0.5 ML of NiO/HOPG. The Ni 3*d* states in NiO are split by the octahedral crystal field produced by the O ions into the t_{2g} and e_g subbands. However, the lack of the apical O at the surface of NiO breaks the symmetry and results in a pyramidal crystal field. This effect produces the additional splitting of the e_g subbands into the z^2 and x^2-y^2 states observed in the (0.5 ML) spectrum in Fig. 2(c). Such splitting has also been theoretically reproduced for the NiO (100) surface using the local density approximation including electron repulsion (LDA+*U*).[14] A similar splitting is observed in the Ni e_g region of the spectrum of the 3 nm NiO nanoparticles in Fig. 2(d).[1] This reduced symmetry effect is enhanced in the NiO nanostructures due to their relatively large surface-to-volume ratio.

TABLE I. Parameters of the cluster model calculation. Δ: charge transfer; *U*: electron repulsion; *pdσ*: *p*-*d* hybridization; *B*, *C*: Racah parameters; 10*Dq*: crystal field; Δ_{pyr}: pyramidal splitting.

Parameters	
Δ=4.0 eV	*B*=0.11 eV
U=7.5 eV	*C*=0.48 eV
pdσ=1.4 eV	10*Dq*=1.0 eV
	Δ_{pyr}=0.6 eV

To corroborate this theory, we have calculated the O 1*s* XAS spectra using cluster model calculations in octahedral and pyramidal symmetries. The main parameters used in the calculation are listed in Table I, and are similar to those suggested by Fujimori *et al.*[5] Figure 3 shows the near-edge region of the O 1*s* XAS spectra of (a) large NiO coverages (bulk), (b) low NiO coverages (0.5 ML), and (c) 3 nm NiO nanoparticles. The background of the spectra was adjusted using an arctan function and Lorentzian curves to simulate the Ni 4*sp* region. The octahedral (bulk) calculation shows a single line (short dash) corresponding to transitions to Ni e_g states; as shown in Fig 3(a) the agreement with the spectrum of bulk NiO is excellent. The pyramidal (surface) calculation presents two lines (short dots) corresponding to the x^2-y^2 and z^2 states. The spectrum of low NiO coverages (0.5 ML) in Fig. 3(b) contains not only the surface components but also a bulk contribution. The bulk contribution in this case is due to the relatively large thickness (3–10 nm) of the NiO islands. Figure 3(c) shows that the spectrum of the 3 nm NiO nanoparticles is well explained just by the surface components, because the surface-to-volume ratio of the nanoparticles is larger than for the NiO islands on HOPG. The excellent

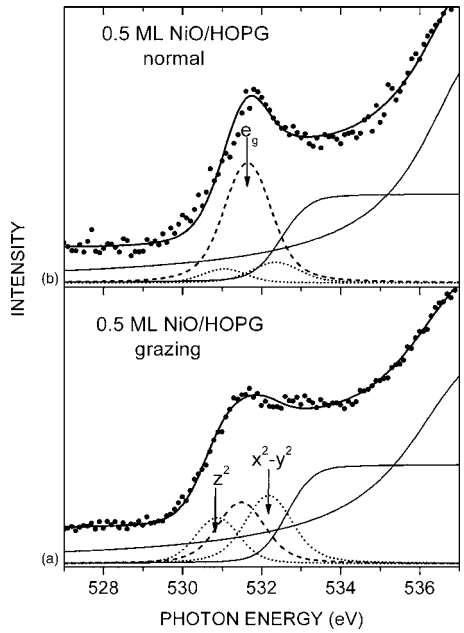

FIG. 4. Calculations and experimental data of the near edge region of the O 1*s* XAS spectra of 0.5 ML NiO/HOPG taken at (a) grazing and (b) normal incidence.

agreement with the calculations confirms the interpretation of the O 1*s* XAS spectrum of the NiO nanoparticles,[1] and strongly suggests that the same splitting mechanism, due to surface effects, is operating in (0.5 ML) NiO/HOPG. Therefore, cluster calculations have confirmed a completely new interpretation of the NiO surface electronic structure in terms of the splitting of the e_g electronic states.

Figure 4 shows the O 1*s* XAS spectra of 0.5 ML NiO/HOPG taken at (a) grazing and (b) normal photon incidence. The spectra exhibit a clear dependence (dichroism) with the relative polarization of the incident light. The normal incidence spectrum, with the electric field E parallel to the surface, resembles that of bulk NiO with a relatively broader single e_g peak (short dash). In particular, the distinct splitting due to surface effects (short dots) is very weak in this spectrum. On the other hand, in the grazing incidence spectrum, with the electric field E perpendicular to the surface, the double peak (x^2-y^2 and z^2) structure (short dots) is clearly observed. The dichroism effect shows that the splitting affects mostly the states perpendicular to the surface, and confirms the idea that the splitting is related to the absence of the apical oxygen at the surface. It is worth noting that, in this case, the z^2 orbital forms a dangling bond perpendicular to the surface. This dangling bond might be related to the enhanced catalytic activity of these large surface-to-bulk ratio NiO nanostructures.

In summary, we studied the electronic structure of the NiO nanostructures formed at the early stages of growth (0.5 ML) of NiO on HOPG. The results have been compared to previous x-ray absorption studies for 3 nm NiO nanoparticles. The Ni 2*p* XAS spectra of the NiO planar islands and the NiO nanoparticles confirm that Ni ions are present in the high-spin Ni^{2+} form. On the other hand, the O 1*s* XAS spectra show a splitting of the e_g band attributed to the lack of the apical O atoms at the surface. Cluster calculations have confirmed that this splitting is caused by the pyramidal coordination of the Ni ions at the surface. Further, note the interpretation of the surface electronic structure, in terms of Ni e_g splitted dangling bonds at the surface, which may promote understanding of the catalytic properties of this material.

We want to thank the support of the CICYT of Spain under Contract No. BFM2003-03277 and the European Union through Contract No. R II 3.CT-2004-506008. Fruitful discussion with G. A. Sawatzky is acknowledged. Two of the authors (A.G. and I.P.) thank the Spanish Ministerio de Educación y Ciencia for financial support through the "Ramón y Cajal" and FPI Programs, respectively. We also thank the staff of BESSY for technical support.

[1] L. Soriano, M. Abbate, J. Vogel, J. C. Fuggle, A. Fernández, A. R. González-Elipe, M. Sacchi, and J. M. Sanz, Chem. Phys. Lett. **208**, 460 (1993).
[2] C. Morant, L. Soriano, J. F. Trigo, and J. M. Sanz, Thin Solid Films **317**, 59 (1998).
[3] P. C. Gravelle and S. J. Teichner, Adv. Catal. **20**, 167 (1969).
[4] J. Hubbard, Proc. R. Soc. London, Ser. A **277**, 237 (1964).
[5] A. Fujimori, F. Minami, and S. Sugano, Phys. Rev. B **29**, 5225 (1984).
[6] G. A. Sawatzky and J. W. Allen, Phys. Rev. Lett. **53**, 2339 (1984).
[7] S. Hüfner, J. Osterwalder, T. Riesterer, and F. Hulliguer, Solid State Commun. **52**, 793 (1984).
[8] G. J. M. Janssen and W. C. Nieuwpoort, Phys. Rev. B **38**, 3449 (1988).
[9] M. J. Tomellini, J. Electron Spectrosc. Relat. Phenom. **58**, 75 (1992).
[10] P. Kuiper, G. Kruizinga, J. Ghijsen, G. A. Sawatzky, and H. Verweij, Phys. Rev. Lett. **62**, 221 (1989).
[11] M. Abbate, F. M. F. de Groot, J. C. Fuggle, A. Fujimori, Y. Tokura, Y. Fujishima, O. Strebel, M. Domke, G. Kaindl, J. van Elp, B. T. Thole, G. A. Sawatzky, M. Sacchi, and N. Tsuda, Phys. Rev. B **44**, 5419 (1991).
[12] A. Freitag, V. Staemmler, D. Cappus, C. A. Ventrice, Jr., K. Al Shamery, H. Kuhlenbeck, and H.-J. Freund, Chem. Phys. Lett. **210**, 10 (1993).
[13] B. Fromme, M. Möller, Th. Anschütz, C. Bethke, and E. Kisker, Phys. Rev. Lett. **77**, 1548 (1996).
[14] S. L. Dudarev, A. I. Liechtenstein, M. R. Castell, G. A. D. Briggs, and A. P. Sutton, Phys. Rev. B **56**, 4900 (1997).
[15] D. Ködderitzsch, W. Hergert, W. M. Temmerman, Z. Szotek, A. Ernst, and H. Winter, Phys. Rev. B **66**, 064434 (2002).
[16] J. M. McKay and V. E. Henrich, Phys. Rev. B **32**, 6764 (1985).
[17] M. A. van Veenendaal and G. A. Sawatzky, Phys. Rev. Lett. **70**, 2459 (1993).
[18] A. R. González-Elipe, J. P. Holgado, R. Alvarez, and G. Munuera, J. Phys. Chem. **96**, 3080 (1992).
[19] L. Soriano, M. Abbate, A. Fernández, A. R. González-Elipe, F. Sirotti, G. Rossi, and J. M. Sanz, Chem. Phys. Lett. **266**, 184 (1997).
[20] D. Alders, F. C. Voogt, T. Hibma, and G. A. Sawatzky, Phys. Rev. B **54**, 7716 (1996).
[21] J. M. Sanz and G. T. Tyuliev, Surf. Sci. **367**, 196 (1996).
[22] M. Sánchez-Agudo, F. Yubero, G. G. Fuentes, A. Gutiérrez, M. Sacchi, L. Soriano, and J. M. Sanz, Surf. Interface Anal. **30**, 396 (2000).
[23] S. Agnoli, M. Sambi, G. Granozzi, J. Schoiswohl, S. Surnev, F. P. Netzer, M. Ferrero, A. M. Ferrari, and C. Pisani, J. Phys. Chem. B **109**, 17197 (2005).
[24] L. Soriano, G. G. Fuentes, C. Quirós, J. F. Trigo, J. M. Sanz, P. R. Bressler, and A. R. González-Elipe, Langmuir **16**, 7066 (2000).
[25] F. M. F. de Groot, J. C. Fuggle, B. T. Thole, and G. A. Sawatzky, Phys. Rev. B **42**, 5459 (1990).
[26] J. van Elp, B. G. Searle, G. A. Sawatzky, and M. Sacchi, Solid State Commun. **80**, 67 (1991).
[27] I. Davoli, A. Marcelli, A. Bianconi, M. Tomellini, and M. Fanfoni, Phys. Rev. B **33**, 2979 (1986).
[28] S. I. Nakai, T. Mitsuishi, H. Sugawara, H. Maezawa, T. Matsukawa, S. Mitani, K. Yamasaki, and T. Fujikawa, Phys. Rev. B **36**, 9241 (1987).
[29] H. L. Skriver, *The LMTO Method* (Springer, Berlin, 1991).
[30] M. Abbate, J. B. Goodkoep, F. M. F. de Groot, M. Grioni, J. C. Fuggle, S. Hofmann, H. Petersen, and M. Sacchi, Surf. Interface Anal. **18**, 65 (1992).